KI REPORTS
KIReports.org
TRANSLATIONAL RESEARCH

Chronic Oral Exposure to Synthetic Amorphous Silica (NM-200) Results in Renal and Liver Lesions in Mice

Delphine Boudard[1,2], Federica Aureli[3], Blandine Laurent[1], Nathalie Sturm[4], Andrea Raggi[3], Emilie Antier[5], Latifa Lakhdar[5], Patrice N. Marche[4], Michèle Cottier[1], Francesco Cubadda[3] and Anna Bencsik[5]

[1]CHU Saint Etienne, UF6725 Cytologie et Histologie Rénale, St-Etienne, France; [2]Université de Lyon, INSERM UMR 1059, Equipe DVH/PIB, Faculté de Médecine St-Etienne, France; [3]Istituto Superiore di Sanità-Italian National Institute of Health, Rome, Italy; [4]U1209 INSERM-Université Grenoble-Alpes, France; and [5]Université de Lyon 1, Anses, Lyon, France

Introduction: Silicon dioxide, produced as synthetic amorphous silica (SAS), is made of nanoparticles (NPs), either present as such or as agglomerates and aggregates, and is widely used in many types of food processes and products as an additive. To assess whether repeated, long-term exposure to SAS NPs may result in adverse effects, mice were exposed for 18 months *via* drinking water to NM-200, one of the reference nanostructured silica used for applications related to food, at 4.8 mg NM-200/kg body weight per day, a dose relevant to the estimated dietary exposure to SAS in humans.

Methods: The experiment focused on the kidney and liver as target organs and was carried out in parallel using 3 mouse lines (wild type and transgenic) differing for the expression of α-synuclein, that is, murine and human mutated (A53T). Sensitive determination of silicon revealed higher contents in liver and kidneys of NM-200–exposed mice compared with unexposed aged-matched controls.

Results: Histological abnormalities, such as vacuolization of tubular epithelial cells, were detected in all kidneys, as well as inflammatory responses that were also detected in livers of exposed animals. Less frequent but more deleterious, amyloidosis lesions were observed in glomeruli, associated with perivascular amyloid accumulation in liver.

Conclusion: These histological findings, in conjunction with the observation of detectable deposition of silica, highlight that chronic oral intake of SAS may pose a health risk to humans and need to be examined further.

Kidney Int Rep (2019) **4,** 1463–1471; https://doi.org/10.1016/j.ekir.2019.06.007
KEYWORDS: chronic oral exposure; E551; kidney; mice; nanoparticles; silica

SAS is widely used as a food additive (E551, according to the European nomenclature of food additives) in many types of food processes and products with different functions, (e.g., to clear beers, to maintain flow properties in powder products, or to thicken pastes). The means of SAS production (wet, i.e., precipitation, and thermal, i.e., pyrogenic) efficiently yields silicon dioxide (SiO_2) nanoparticles (NPs) (i.e., sized <100 nm),[1] which can be then variably agglomerated and aggregated depending on the conditions of production and use.[2–8] The primary NPs present in the food additive E551 may partly bind to form agglomerates in the food matrix, but after gastrointestinal digestion, the gut epithelium appears to be predominantly exposed to nanosized silica.[4,9–12] Consumer intake of silica from food was estimated to be at 9.4 mg/kg body weight per day for the adult Dutch population, of which 1.8 mg/kg body weight per day was estimated to be in the nano-size range.[12] The consequences for humans of daily and long-term exposure to nanoparticulate materials remain essentially unknown. There is only limited information about the impact of oral exposure to SAS NPs on human health. Whereas several *in vitro* studies showed a number of adverse effects, dependent on particle size and type, and mainly mediated by oxidative stress and release of proinflammatory cytokines, less information is available *in vivo* and specifically dealing with the oral route of exposure.[4,13–16] Biodistribution of SAS NPs is mainly directed at liver, kidneys, spleen, and lungs,

Correspondence: Anna Bencsik, French Agency for Food, Environmental and Occupational Health and Safety (ANSES), 31 Avenue Tony Garnier, 69364 Lyon, France. E-mail: anna.bencsik@anses.fr

Received 9 June 2019; accepted 10 June 2019; published online 22 June 2019

whereas the liver appears to be the target organ for toxicity (Cubadda F, Oomen AG, Laurentie M, *et al.*, unpublished data, 2019).[14,17–20] A recent subchronic toxicity study in rats orally exposed to different food-grade SAS types documented a decrease in gastrointestinal absorption at higher dose levels; this was related to gelation that occurs when silica is dispersed at high concentration and highlights the necessity to test lower doses.[19] However, very high dose levels have been used in all available oral studies,[21–24] making their significance questionable for human risk assessment of engineered nanomaterials in general, and specifically of SAS NPs.[14] Overall, given the large use of SAS in the food sector as well as very limited data on oral exposure, the effects of ingestion of low doses for a long period do represent an important knowledge gap and urgent need of research. A recent risk assessment of E551 in food, which used an internal dose approach to deal with the potential for accumulation in tissues with daily consumption, concluded that SAS NPs in food may pose a health risk.[14]

The aim of the present study was to assess potential adverse effects of long-term oral exposure to a low dose of SAS NPs and focused on kidneys and liver, organs involved in detoxification and elimination, and thus main potential targets. The selected material NM-200 is a precipitated SAS that has been characterized in previous studies and tested in the Organisation for Economic Co-operation and Development (OECD) program on engineered nanomaterials safety as one of the reference nanostructured silica used for applications related to food.[3] Most oral toxicity studies are based on gavage administration of NPs, but for longer-term experiments, animals are often exposed through their drinking water, as recently reported in investigations on food-grade TiO_2 NPs, for example.[25] In the present study, mice were exposed to SAS NPs continuously, for 18 months, through their drinking water. There is no *in vivo* study available that investigated such a long-term exposure. The experiment was carried out in parallel using 2 different wild-type mouse lines, namely C57BL/6 and C57BL/6S. Besides, a 9-month exposure study was performed in a transgenic mouse line (TgHuA53T) expressing the human mutated (A53T) α-synuclein protein. Mice of each line exposed to tap water without NPs were used as controls. Here we report the findings of histological examination of kidneys and livers, and document silica deposition in both organs using highly sensitive inductively coupled plasma mass spectrometry detection.

METHODS

Nanomaterial

The engineered nanomaterial used in this study, namely NM-200, is an industrially manufactured, precipitated SAS with a primary particle size of approximately 20 nm, mainly used for food processing. A thorough physicochemical characterization of this material has been published previously[3] and the main characteristics of this NM-200 are given in Supplementary Table S1.

Stock suspensions of NM-200 were prepared using the standardized dispersion protocol developed in the Nanogenotox Joint Action (www.nanogenotox.eu)[26,27] (see Supplementary Methods). The freshly dispersed NM-200 stock suspension was diluted with tap water to reach a final concentration of 30 mg L^{-1}. The particle size distribution of the final suspension administered to mice was characterized by asymmetric flow-field flow fractionation–inductively coupled plasma mass spectrometry. The method used, as well as the results, are given in the Supplementary Materials.

Ethics of Animal Experiments

The experimental study was conducted according to the guidelines laid down by the French Ethical Committee (Decree 87–848) and European Community Directive 86/609/EEC. The chronic oral exposure protocol was approved (11–0042) by the French Agency for Food, Environmental and Occupational Health and Safety (ANSES)/ENVA/UPEC ethics committee (National Committee on the Ethics of Animal Experiments). Animal experiments were performed in the ANSES animal facilities, which have the relevant approval to carry out animal work (C 69 387 0801) by licensed people working in the animal experiment unit (license numbers AB: 69 387 531, LL: 69 387 191). These facilities have the advantage of the greatest experience in long-term studies, with an ability to manage aging animals. Several years of experience in the field of prion diseases allowed standardizing and optimizing the experimental conditions in which groups of mice can be followed for 1 to 3 years.[28,29]

Study Design

The experimental design is reported in detail in the supplementary information. Because of the long duration of the study, the mouse lines C57BL/6 (Charles River, Ecully, France) and C57BL/6S[30] (Harlan, Gannat, France), were selected on the criteria of absence of any spontaneous diseases, in particular no kidney or liver tumors that could appear with natural aging. Groups of 5 to 8 female mice, 3 months old at the beginning of the experiment (average weight 20 to 25 g), were exposed orally to NPs through their drinking water for 18 months. Control group of each mouse line ($n = 7$ and $n = 8$) received only tap water during the 18 months. A third experiment (see details in Supplementary Methods and Supplementary Figure S1) was set up

using a transgenic mouse model, expressing the human mutated (A53T) α-synuclein protein (TgHuA53T),[31,32] to study the impact of 3-, 6-, and 9-month exposure to silica in drinking water on young (8 weeks old, average weight 20 to 25 g) transgenic mice ($n = 15$, male and female) compared with the matched controls ($n = 10$, unexposed transgenic mice).

Necropsy

Mice of each group were killed after 18 months of exposure to NM-200, by an i.p. injection of pentobarbital (200 μl–54.7 mg/ml). Necropsy was performed under strict clean room conditions, and organs were collected and either frozen or fixed to determine silica content or to perform histopathological studies.

Total Silicon Determination in Tissues

All procedures are described in detail in the Supplementary Methods and were carried out under clean room conditions to avoid any contamination. Total silicon concentrations were determined by means of an Agilent (Santa Clara, CA) 8800 ICP-QQQ mass spectrometer. Optimized analytical conditions for accurate Si detection by inductively coupled plasma mass spectrometry have been reported elsewhere.[33] Quantitative determinations were carried out by the method of standard addition. Trueness was assessed by the analysis of the internal quality control material ISS-BL, a bovine liver sample spiked with soluble silicon, with a reference value for Si of 20.4 ± 1.9 μg/g (Aureli F, D'Amato M, Raggi A, *et al.*, unpublished data, 2019), which was included in each analytical batch. The average determined Si concentration was 19.1 ± 1.7 μg/g ($n = 4$), in good agreement with the target value. Statistical analyses for tissue silicon content were carried out comparing exposed to control groups by means of the Mann-Whitney U test. Statistical analyses were performed with SPSS Statistics Version 19 (IBM, Armonk, NY).

Histopathology

Liver and kidney preparations are provided in detail in the Supplementary Methods (Supplementary Figure S2). Different kidney colorations were performed on sagittal sections (0.5- to 3-μm-thick) representative of the whole kidney; the 3-μm-thick sections were stained with Masson Trichrome coloration, 2-μm-thick sections with periodic acid–Schiff (PAS) and 0.5-μm-thick sections with a silver impregnation. The combination of these stainings was used to evaluate the size and appearance of glomeruli, cortical and distal renal tubules, and interstitial tissue with blood vessels; altogether, these morphological aspects were evaluated by a nephropathologist using an Olympus (Tokyo, Japan) BX51 microscope coupled with an Olympus DP12 camera, and scored as follows: Grade 1, for 0% to 25% of lesions observed in the section (+); Grade 2, for 25% to 50% of lesions observed in the section (++); Grade 3, when there was more than 50% of lesions in the section (+++).

The other half kidneys were used to characterize in-depth findings suggestive of amyloidosis. Sagittal frozen sections, 4 μm thick, were stained with Crystal Violet, Congo Red, or used for immunodetection of several proteins of interest, using specific antibodies against IgM, IgG, kappa and lambda chains, beta amyloid, and serum amyloid A (SAA) protein (Supplementary Table S2). Evaluation of immunostaining intensity was performed using a scoring scale defined as follows: negative, low (+), intermediate (++), and high (+++) expression, giving in addition the localization of the staining in the nephron segment. Liver and kidney complementary results are provided in the Supplementary Data (Supplementary Table S3).

Kidney Function

At the time the study on wild-type mice was designed, adverse effects on kidney function were unforeseen and this endpoint was not evaluated. However, when the first histopathological observations were made, a urine test was included in the ongoing study in transgenic mice (TgHuA53T). Proteinuria was monitored weekly by dipstick urinalysis (Albustix; Siemens, Munich, Germany) (see Supplementary Methods and Data, Supplementary Table S4, and Supplementary Figures S3 and S4).

RESULTS

No mortality, no treatment-related effects on animal body weight, body weight gain, or tissue weights were detected in wild-type mice. No abnormal signs in mice behavior were observed during the experiment.

Silica Deposition in NM-200–Exposed Mice

To be able to detect the minute amounts of deposited silica resulting from chronic administration of low doses, relevant to human exposure, an advanced analytical methodology was used to deal with the spectral interferences in the ICP-MS determination of silicon (Aureli F, D'Amato M, Raggi A, *et al.*, unpublished data, 2019).[8,33,34] By using a fit-for-purpose method based on the use of state-of-the-art inductively coupled plasma mass spectrometry technology, extremely low limits of detection could be achieved and tissue silica levels could be accurately determined (as silicon) in both control and treated animals (Figure 1). In kidney, silica levels were higher in C57BL/6 mice compared with both C57BL/6S mice and

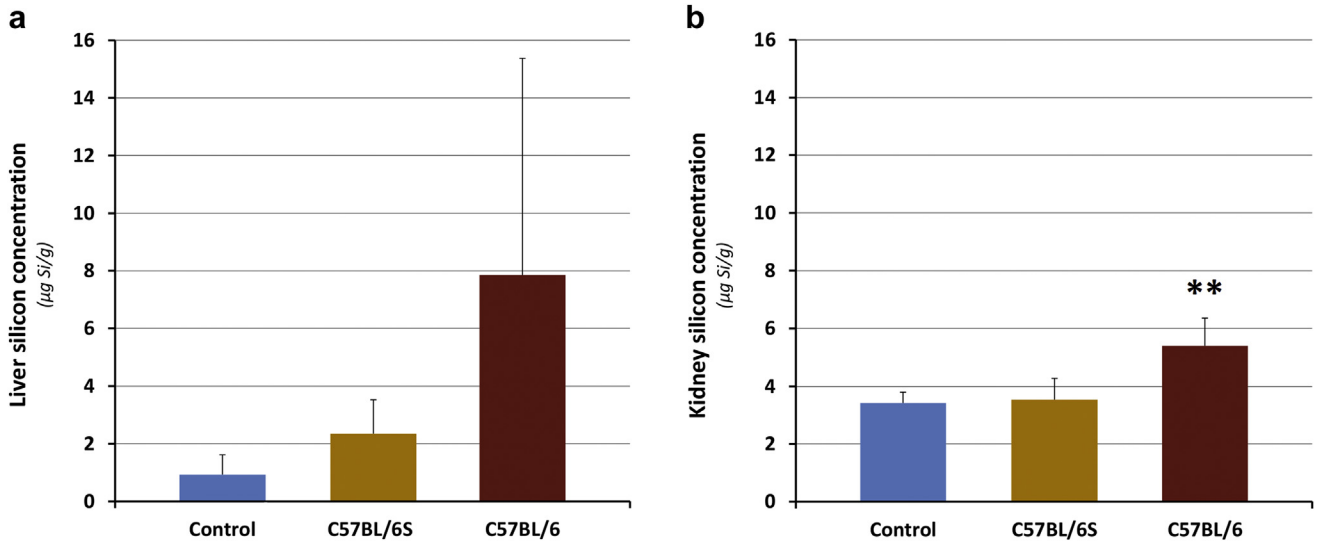

Figure 1. Silicon tissue concentration after 18 months of treatment in the (a) liver and (b) kidney. Concentrations in µg/g of fresh tissue ($n = 4$–7 for exposed mice, $n = 4$–6 for control mice). **Statistically significant difference compared to both Control and C57BL/6S ($P < 0.01$).

controls (statistically significant, $P < 0.01$). Silica deposition in liver followed the order C57BL/6 mice > C57BL/6S mice > control mice, although with a high interindividual variability. The silica concentration was higher in livers compared with kidneys of C57BL/6 mice (Figure 1). These tissue levels at the end of the treatment might have been the result of a more efficient absorption and distribution of silica NPs in C57BL/6 mice or more likely, a higher retention in tissues, due to less efficient elimination.

Histopathological Changes in Kidneys in NM-200–Exposed Mice

No morphological abnormalities were noted on young adult or age-matched control mice (not exposed to NPs, Figure 2a and b), but several histo-morphological

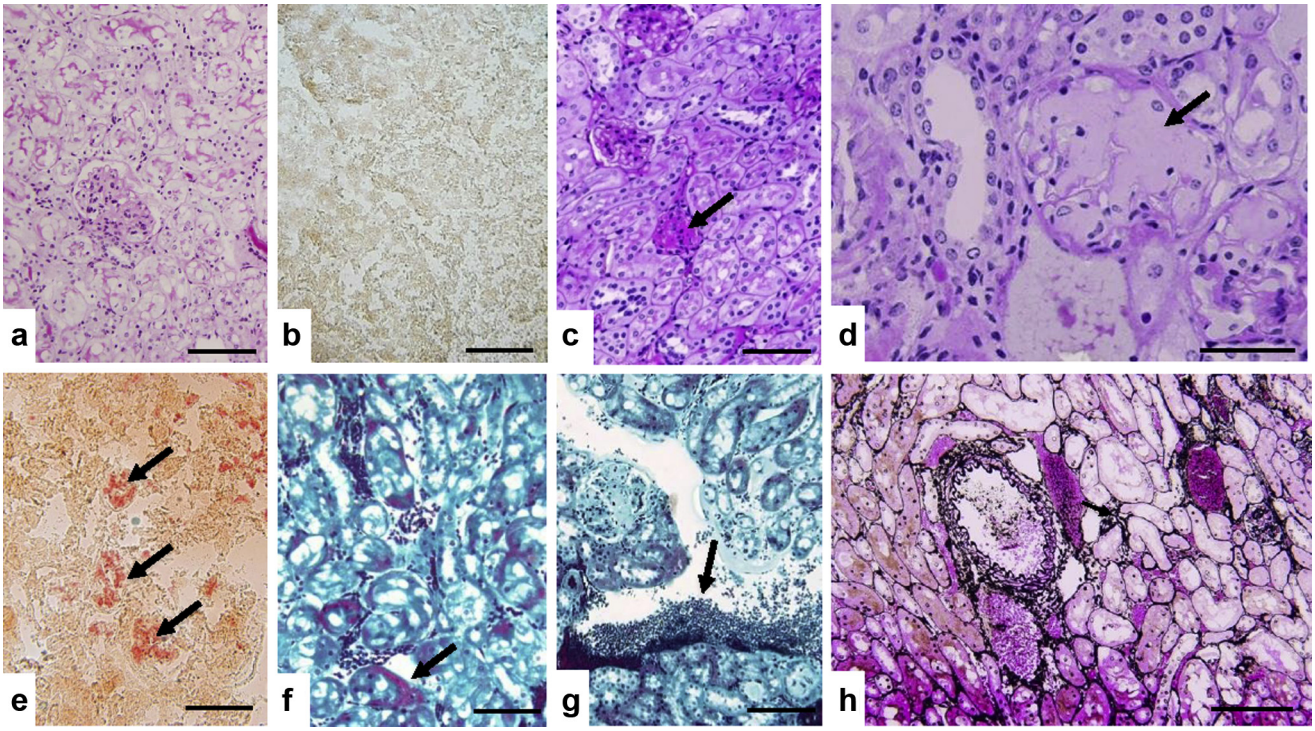

Figure 2. (a, b) The unexposed C57BL/6 mouse aged-matched control shows normal histological morphology of the kidney (a, periodic acid–Schiff [PAS] stain) without amyloidosis (b, Red Congo stain). (c–e) Glomerular abnormalities observed in the C57BL/6 mouse exposed to synthetic amorphous silica nanoparticles with hyaline deposits (c, arrow, PAS stain), and pale amorphous amyloidosis deposition in glomeruli (d, arrow, PAS stain) confirmed by positive Red Congo staining (e, arrow). (f, g) Masson Trichrome staining shows, respectively, dilated peritubular capillaries (f, arrow) and perivascular lymphoid infiltrates (g, arrow). (h) Representative of silver impregnation that illustrates the absence of atrophic lesions or tubular necrosis. Bars = 200 µm (b, c, e, f, h), 100 µm (a, g), and 50 µm (d).

Table 1. Summary of the histopathological changes observed in the kidney of mice after 18-month exposure to SAS NM-200 via drinking water

		Kidney histopathological changes				
Exposure	**Mouse line**	**Glomerulus**	**Glomerulus amyloid status**	**Tubules**	**Interstitial tissue**	**Blood vessels**
Control group exposed to tap water without NPs	C57BL/6S ($n = 6$) old C57BL/6 ($n = 7$) old and ($n = 9$) young adult	No abnormalities No abnormalities	No abnormalities No abnormalities	No abnormalities No abnormalities	No abnormalities No abnormalities	No abnormalities No abnormalities
SiO_2-NPs	C57BL/6S ($n = 5$)	Focal and segmented hyaline deposits + (1/5) No amyloidosis	No abnormalities	Vacuolization of the tubular epithelial cells without atrophic lesions or necrosis (5/5)	Perivascular lymphoid infiltrates + (4/5), often with dilated peritubular capillaries (2/5)	No abnormalities
	C57BL/6 ($n = 3$)	Focal and segmented hyaline deposits + (1/3) weakly acellular amorphous deposits PAS +++ on all glomeruli (1/3)	Amyloid glomeruli were all positively stained +++ (1/3) βamyloid neg IgG pos + IgM pos ++ λ chain pos + κ chain neg	Vacuolization of the tubular epithelial cells without atrophic lesions or necrosis (3/3)	Perivascular lymphoid infiltrates + (2/3) ++ (1/3)	No abnormalities

neg, negative; NP, nanoparticle; PAS, periodic acid–Schiff; pos, positive; SiO_2, silicon dioxide.
The scoring of lesion extend is + (0%–25%), ++ (25%–50%), and +++ (more than 50%). Amyloid status was confirmed with immunostainings in the only C57BL/6 mice showing PAS morphological amyloid glomeruli.

alterations were identified in kidneys of exposed mice (Table 1, Figure 2c–h). Regarding interstitial tissue, as shown in Figure 2g, lymphoid infiltrates were observed quoted + (two-thirds of specimens) to ++ (one-third of specimens) for C57BL/6 mice, whereas C57BL/6S specimens exhibited 4 of 5 lymphoid infiltrates quoted + often with perivascular localization but without edema or fibrosis. Lymphoid infiltration was also associated in 2 of 5 C57BL/6S samples with dilated peritubular capillaries with intrinsic erythrocytes (Figure 2f). Vacuoles within tubules, especially proximal tubules, were seen in all the animals exposed to NM-200 whatever the mouse line, without atrophic lesions or tubular necrosis (Figure 2h). The more deleterious observations concerned glomeruli. Indeed, typical homogeneous, glassy appearance of the glomerular cytoplasm revealed the presence of focal and/or segmented hyaline deposits for 1 of 5 C57BL/6S mice and 1 of 3 C57BL/6 mice (Table 1, Figure 2c). Moreover, PAS pale amorphous amyloid deposits were identified in 1 of 3 of C57BL/6 exposed mice (Table 1, Figure 2d), whereas they were absent in the 5 available kidneys of the exposed C57BL/6S mice as well as in control animals. Amyloidosis observed on the basis of PAS morphological observations have been confirmed by means of Crystal Violet and especially Congo Red–specific colorations, as shown in Figure 2e. The amyloidosis type was further investigated with immunostaining against several proteins of interest, that is, beta amyloid protein, IgG and IgM, kappa and lambda chains, completed with SAA protein. As summed up in Table 1 and shown in Figure 3, a significant IgM staining ++ was observed for the only specimen exhibiting amyloidosis deposits, associated promptly with IgG + and lambda + chains immunostaining, but without concomitant expression of kappa chains. This case also showed a positive SAA immunostaining in glomeruli and vascular sections (Figure 3g). These results support the presence of combined light-chain (AL) and SAA amyloidosis.

Histopathological abnormalities in livers from NM-200–exposed mice are provided in detail in Supplementary Table S3 and Supplementary Figure S2.

To sum up, long-term oral exposure of mice to silica NM-200 through drinking water triggered renal and liver inflammation and resulted in lesions, for example, vacuolization of tubular epithelial cells (detected in 100% of the kidneys), including SAA amyloidosis in C57BL/6 mice.

Considering liver and kidney histopathological observations, the C57BL/6S line of mice, which differs from the C57BL/6 line solely by the lack of α-synuclein expression, showed fewer lesions. The fact that the control mice (young or aged-matched) did not show these lesions indicates that these histological changes are not related to normal aging and rather appeared to be treatment-related.

Alteration of Kidney Function in NM-200–Exposed Mice

Proteinuria, monitored weekly in transgenic mice (TgHuA53T)[31,32] since the third month of exposure (Supplementary Table S4), showed some interindividual and time-dependent variability. However, the rate of 1 g/l, revealing clear proteinuria, was definitely more frequent in exposed mice compared with controls ($P < 0.001$). In addition, only mice from exposed groups showed a pathological rate of 3 g/l, reflecting

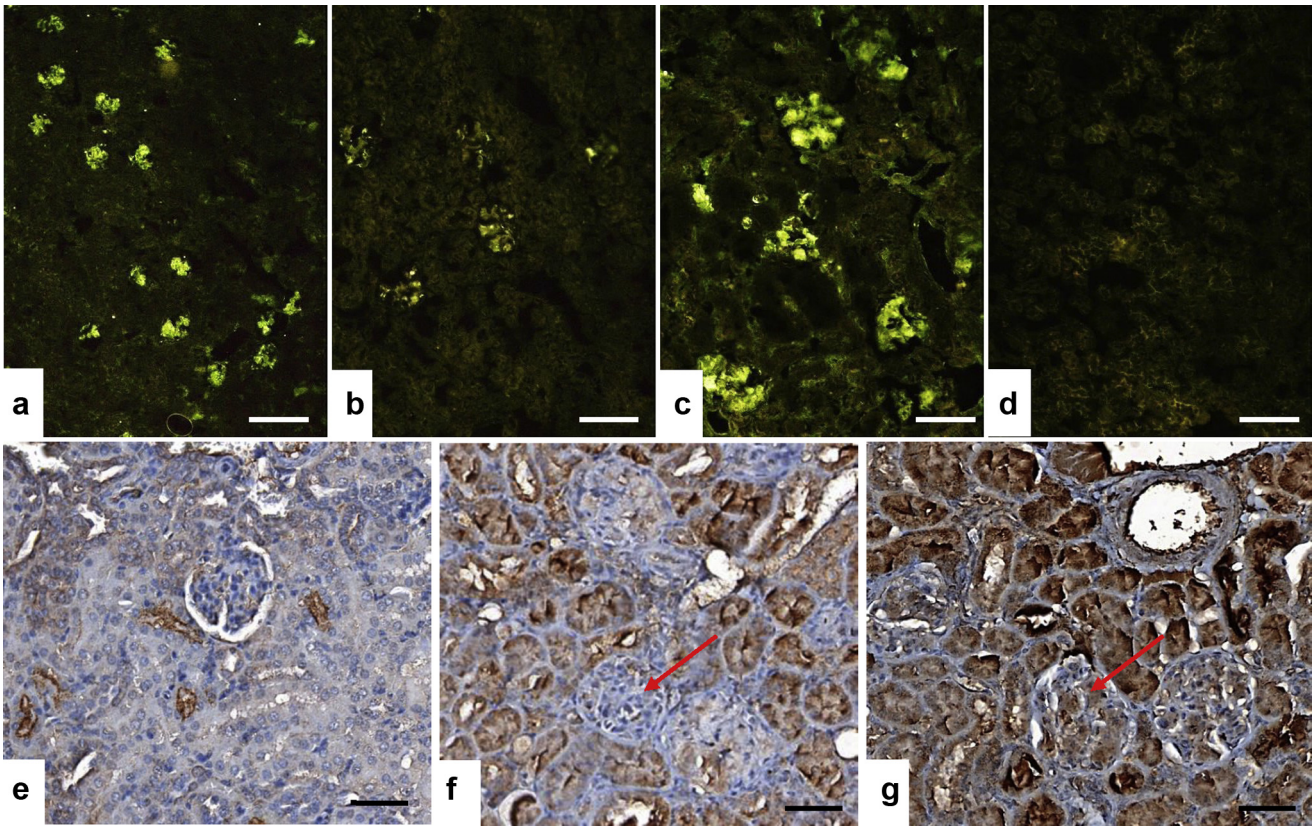

Figure 3. Immunological characterization: (a) IgM, (b) IgG, (c) λ chain, and (d) κ chain of glomerular amyloidosis in the C57BL/6 mouse exposed to synthetic amorphous silica (SAS) nanoparticles (NP) for 18 months. A significant IgM staining scored ++ was recovered for the only mouse (1 of 3 C57BL/6) exhibiting morphological periodic acid–Schiff glomerular abnormalities that was associated with IgG + and lambda chain+ expression levels. (e) On the kidney of the C57BL/6S mouse exposed to SAS NP showing no amyloidosis, only background serum amyloid A (SAA) staining was observed. (f) On the amyloid kidney of the C57BL/6 mouse exposed to SAS NP, the internal immunohistochemical negative control in which the SAA primary antibody was replaced by the diluting solution revealed nonspecific stainings on the tubular sections and no SAA-specific immunoreactivity in glomeruli (red arrow). (g) On the kidney of the C57BL/6 mouse exposed to SAS NP diagnosed with amyloidosis, a specific SAA immunoreactivity was detected (brown deposits) in the glomeruli (red arrows). Bars = 400 μm (a), 200 μm (b), 100 μm (c), 200 μm (d), and 50 μm (e–g).

renal insufficiency. Silica levels in kidneys of treated TgHuA53T transgenic mice were higher than controls ($P < 0.05$) (Supplementary Figure S3). Tubular alterations, with diffuse presence of vacuoles, were found in the kidneys of mice after 6 months of exposure (Supplementary Figure S4), without evidence of glomerular amyloidosis. These histological alterations might be consecutive to the obvious 3-month silica deposition. Even in the absence of glomerular alterations, proteinuria may, however, be an indication of glomerular dysfunction in the context of a nephrotic syndrome without, at this stage, significant histological alterations.

In this experiment, mortality was detected before the sixth month of exposure compared with controls.

DISCUSSION

Even though SAS has been used as food additive for decades, its safety has been only recently investigated with specific attention to the nanoparticulate nature of the material.[14] Taking into account the latter and the potential for accumulation in tissues with daily consumption, a recent nano-specific risk assessment highlighted that more insight in the health risk of SAS in food is warranted.[14] Evidence to date suggests that liver is the target organ of toxicity of ingested or intravenously injected nanosized silica (histopathological findings include fibrosis and granulomas) and that long-term studies at relevant low doses are critical to address the potential risks for human health arising from daily lifelong dietary exposure.[14,19] However, to our knowledge there are no studies investigating long-term exposure to dietary SAS.

The present study provides new evidence that daily exposure for 18 months to low levels of SAS as NM-200, using a dosage (4.8 mg SiO_2/kg body weight per day) relevant to human dietary exposure, leads to deposition of detectable amounts of silica in kidney and liver. This accumulation in tissues is associated to histopathological alterations in kidney and liver that can be severe, as in the case of amyloidosis observations. Although not present in all the animals, these

alterations should be considered seriously, especially as the most severe lesions are not seen in any of the control groups followed in parallel.

We focused on kidney and liver for their relevance when dealing with oral chronic exposure and based on evidence that they are target organs for nanosilica distribution, with liver especially appearing key (Cubadda F, Oomen AG, Laurentie M, *et al.*, unpublished data, 2019).[14,17–20] The present work shows that long-term exposure to low doses of SAS NPs in drinking water leads to histological abnormalities in both organs, unrelated to normal aging, that were characterized by a vacuolization of tubular epithelial cells, detected in 100% of the kidneys, along with renal and liver inflammation accompanied at times by amyloidosis in kidney glomeruli and in perivascular regions in livers.

To the best of our knowledge, in nanomaterial toxicology, the type of lesions observed in the present study, have never been reported before. In the kidney of exposed animals, the morphological modifications of renal tubular cells suggest an epithelial alteration that can still be considered reversible at this stage, due to the absence of observable tubular necrosis. The presence of lymphoid infiltrates with dilated peritubular capillaries suggests, however, the development of an interstitial inflammatory process, resulting in parenchymal tissue alterations that take a progressively chronic character, compatible with the long duration of exposure. The most severe lesions, as they are not reversible, have been observed within the glomeruli with the presence of hyalinosis (1 case respectively for C57BL/6 and C57BL/6S mouse lines), and mostly for the amyloidosis C57BL/6 mouse case. Similarly, the liver was associated with amyloidosis only in the C57BL/6 mouse line (3 cases of 6, including the 1 showing amyloidosis in kidneys). Taking into account amyloidosis occurrence, it is difficult to distinguish the 2 mouse lines in terms of expression of such a pathological response. The difference between the 2 mouse lines is α-synuclein expression; had silica NPs tended to favor the aggregation of α-synuclein proteins as described in the case of gold NPs,[35] a clear difference would have been identified. However, no evidence of any amyloid deposits made of α-synuclein could be highlighted in exposed mice (data not shown). This was confirmed by the use of the third mouse line, expressing a human mutated form of α-synuclein, and for this reason prone to adopt an amyloid form, in particular in the presence of some chemical products able to trigger a neurodegenerative process (e.g., pesticides).[36] Altogether, these observations reveal that precipitated SAS, in the form of NM-200, is a potential risk factor in the promotion of liver and renal amyloidosis unrelated to α-synuclein. Amyloidosis is a common cause of glomerular damage aside from other immune complex glomerular diseases leading eventually to a severe alteration of the glomerular filtration barrier, and therefore ultimately of the renal function.[37] In practice, there are 3 major forms of amyloidosis: AL (amyloid light chain), AA (serum amyloid A protein), and amyloidosis caused by transthyretin, different from those affecting the brain that result in distinct diseases. The AL type is characterized by the deposition of Ig complexes (light chains in most cases), the AA type by a greatly increased concentration of SAA protein in a chronic inflammatory context; the amyloidosis caused by the transthyretin type (genetic) involves the protein transthyretin and is characterized by neuropathies as well as cardiomyopathy.

In our study, the first step to differentiate between AL and AA amyloidosis performed by immunodetection of Ig light chains suggested a possible AL amylose type with the expression of IgM associated more specifically with lambda Ig chain. The combined expression on the one hand of light Ig chains and on the other hand of protein SAA, oriented toward a predominant diagnosis of AA amyloidosis. Indeed, in humans, even if this appears to be rare, some cases diagnosed as AA amyloidosis have also been reported to exhibit staining for light chains. These Ig light chains could be "trapped" in the amyloid deposits leading to misinterpretation of staining patterns.[38,39]

The presence of amyloidosis is interesting in the context of a group of human diseases that, despite being probably underdiagnosed,[40] occur with a prevalence of approximately 20 per million inhabitants in Western countries[41] and whose precise etiology is unknown,[37,42] as well as in relation to chronic kidney diseases.[43,44] Besides a chronic inflammatory state, several largely unknown factors contribute to the appearance of these diseases. Our study suggests that nanostructured elements present in the diet might be one of them. In humans, a high level of silica in water has been suggested as 1 of the possible factors explaining the rampant cases of chronic kidney disease of unknown etiology observed in the Uddanam area of India.[45] In humans, many authors suggested that young adult men are more prone to severe chronic kidney disease of unknown etiology than women. In our animal model, the existence of a sex difference, with higher sensitivity of males compared with females, cannot be excluded. In the transgenic line, males appeared more prone to proteinuria. Altogether, these results show that chronic exposure to dietary SAS may pose a health risk to humans and warrant targeted studies to characterize the dose-response relationship for the observed adverse effects.

DISCLOSURE

All the authors declared no competing interests.

ACKNOWLEDGMENTS

The authors dedicate this paper to our late collaborator, Brigitte Roman. She was an excellent technical assistant. The authors thank Mikael Leboidre for histotechnological assistance as well as the members of the *Plate-forme d'expérimentation animale* at ANSES Lyon (Animal Facilities) for their contribution to the mouse experiments and the team of the Pathology Research Plateform, Department of Translational Research and Innovation, Centre Léon Bérard, Lyon, France for their excellent histotechnological assistance in AA diagnosis.

SUPPLEMENTARY MATERIAL

Supplementary File (PDF)

Supplementary Methods.

Table S1. Main physicochemical characteristics of SAS NM-200.[a]

Table S2. List of antibodies used for amyloidosis characterization by immunohistochemistry.

Table S3. Summary of the histopathological changes observed in the liver of mice after 18-month exposure to SAS NM-200 via drinking water. The lesion scoring was recorded using a 3 grade system: 0 (absent), + (minimal), and ++ (marked). Steatotic-like cytoplasmic vacuolization and inflammation were semi-quantified as 0 (absent), + (minimal), and ++ (marked) for cytoplasmic vacuolization, and 0/(+) (absent or not more than 1 inflammatory foci without apoptotic body and without more than 10 inflammatory cells in the overall cut section), + (few inflammatory foci), and ++ (numerous inflammatory foci) for inflammation.

Table S4. Proteinuria changes in kidneys from NM-200–exposed transgenic mice.

Supplementary Data Set.

Figure S1. Schematic view of the experimental design.

Figure S2. Histopathological changes in livers from NM-200–exposed mice.

Figure S3. Tissue Si deposition in transgenic mice.

Figure S4. Histopathological changes in kidneys from NM-200–exposed transgenic mice.

Supplementary References.

REFERENCES

1. Bouwmeester H, Brandhoff P, Marvin HJP, et al. State of the safety assessment and current use of nanomaterials in food and food production. *Trends Food Sci Technol*. 2014;40:200–210.
2. Yang Y, Faust JJ, Schoepf J, et al. Survey of food-grade silica dioxide nanomaterial occurrence, characterization, human gut impacts and fate across its lifecycle. *Sci Total Environ*. 2016;565:902–912.
3. Rasmussen K, Mech A, Mast J, et al. *Synthetic Amorphous Silicon Dioxide (NM-200, NM-201, NM-202, NM-203, NM-204): Characterisation and Physico-Chemical Properties. JRC Scientific and Technology Reports*. Luxembourg: Euoropean Commission; 2013.
4. Dekkers S, Bouwmeester H, Bos PM, et al. Knowledge gaps in risk assessment of nanosilica in food: evaluation of the dissolution and toxicity of different forms of silica. *Nanotoxicology*. 2013;7:367–377.
5. De Temmerman PJ, Van Doren E, Verleysen E, et al. Quantitative characterization of agglomerates and aggregates of pyrogenic and precipitated amorphous silica nanomaterials by transmission electron microscopy. *J Nanobiotechnology*. 2012;10:24.
6. Contado C, Mejia J, Lozano Garcia O, et al. Physicochemical and toxicological evaluation of silica nanoparticles suitable for food and consumer products collected by following the EC recommendation. *Anal Bioanal Chem*. 2016;408:271–286.
7. Barahona F, Ojea-Jimenez I, Geiss O, et al. Multimethod approach for the detection and characterisation of food-grade synthetic amorphous silica nanoparticles. *J Chromatogr A*. 2016;1432:92–100.
8. Aureli F, D'Amato M, De Berardis B, et al. Investigating agglomeration and dissolution of silica nanoparticles in aequous suspensions by dynamic reaction cell inductively coupled plasma-mass spectroscopy in time resolved mode. *J Anal At Spectrom*. 2012;27:1540–1548.
9. Peters R, Kramer E, Oomen AG, et al. Presence of nano-sized silica during in vitro digestion of foods containing silica as a food additive. *ACS Nano*. 2012;6:2441–2451.
10. Lim JH, Sisco P, Mudalige TK, et al. Detection and characterization of SiO2 and TiO2 nanostructures in dietary supplements. *J Agric Food Chem*. 2015;63:3144–3152.
11. Heroult J, Nischwitz V, Bartczak D, et al. The potential of asymmetric flow field-flow fractionation hyphenated to multiple detectors for the quantification and size estimation of silica nanoparticles in a food matrix. *Anal Bioanal Chem*. 2014;406:3919–3927.
12. Dekkers S, Krystek P, Peters RJ, et al. Presence and risks of nanosilica in food products. *Nanotoxicology*. 2011;5:393–405.
13. Winkler HC, Suter M, Naegeli H. Critical review of the safety assessment of nano-structured silica additives in food. *J Nanobiotechnol*. 2016;14:44.
14. van Kesteren PC, Cubadda F, Bouwmeester H, et al. Novel insights into the risk assessment of the nanomaterial synthetic amorphous silica, additive E551, in food. *Nanotoxicology*. 2015;9:442–452.
15. Napierska D, Thomassen LC, Lison D, et al. The nanosilica hazard: another variable entity. *Part Fibre Toxicol*. 2010;7:39.
16. Jaganathan H, Godin B. Biocompatibility assessment of Si-based nano- and micro-particles. *Adv Drug Deliv Rev*. 2012;64:1800–1819.
17. Yu Y, Li Y, Wang W, et al. Acute toxicity of amorphous silica nanoparticles in intravenously exposed ICR mice. *PLoS One*. 2013;8:e61346.
18. Yu T, Hubbard D, Ray A, et al. In vivo biodistribution and pharmacokinetics of silica nanoparticles as a function of geometry, porosity and surface characteristics. *J Control Release*. 2012;163:46–54.

19. van der Zande M, Vandebriel RJ, Groot MJ, et al. Sub-chronic toxicity study in rats orally exposed to nanostructured silica. *Part Fibre Toxicol*. 2014;11:8.
20. Lee JA, Kim MK, Paek HJ, et al. Tissue distribution and excretion kinetics of orally administered silica nanoparticles in rats. *Int J Nanomedicine*. 2014;9(Suppl 2):251–260.
21. Wolterbeek A, Oosterwijk T, Schneider S, et al. Oral two-generation reproduction toxicity study with NM-200 synthetic amorphous silica in Wistar rats. *Reprod Toxicol*. 2015;56:147–154.
22. So SJ, Jang IS, Han CS. Effect of micro/nano silica particle feeding for mice. *J Nanosci Nanotechnol*. 2008;8:5367–5371.
23. Hofmann T, Schneider S, Wolterbeek A, et al. Prenatal toxicity of synthetic amorphous silica nanomaterial in rats. *Reprod Toxicol*. 2015;56:141–146.
24. Buesen R, Landsiedel R, Sauer UG, et al. Effects of SiO(2), ZrO(2), and BaSO(4) nanomaterials with or without surface functionalization upon 28-day oral exposure to rats. *Arch Toxicol*. 2014;88:1881–1906.
25. Bettini S, Boutet-Robinet E, Cartier C, et al. Food-grade TiO2 impairs intestinal and systemic immune homeostasis, initiates preneoplastic lesions and promotes aberrant crypt development in the rat colon. *Sci Rep*. 2017;7:40373.
26. Schmid K, Riediker M. Use of nanoparticles in Swiss Industry: a targeted survey. *Environ Sci Technol*. 2008;42:2253–2260.
27. Jensen KA, Kembouche Y, Christiansen E, et al. Towards a method for detecting the potential genotoxicity of nanomaterials. Final protocol for producing suitable manufactured nanomaterial exposure media. The generic NANOGENOTOX dispersion protocol–standard operation procedure (SOP) and background documentation. October, 2011. Available at: https://www.anses.fr/en/system/files/nanogenotox_deliverable_5.pdf. Accessed July 10, 2019.
28. Cordier C, Bencsik A, Philippe S, et al. Transmission and characterization of bovine spongiform encephalopathy sources in two ovine transgenic mouse lines (TgOvPrP4 and TgOvPrP59). *J Gen Virol*. 2006;87:3763–3771.
29. Bencsik A, Leboidre M, Debeer S, et al. Unique properties of the classical bovine spongiform encephalopathy strain and its emergence from H-type bovine spongiform encephalopathy substantiated by VM transmission studies. *J Neuropathol Exp Neurol*. 2013;72:211–218.
30. Specht CG, Schoepfer R. Deletion of the alpha-synuclein locus in a subpopulation of C57BL/6J inbred mice. *BMC Neurosci*. 2001;2:11.
31. Giasson BI, Duda JE, Quinn SM, et al. Neuronal alpha-synucleinopathy with severe movement disorder in mice expressing A53T human alpha-synuclein. *Neuron*. 2002;34:521–533.
32. Bencsik A, Muselli L, Leboidre M, et al. Early and persistent expression of phosphorylated alpha-synuclein in the enteric nervous system of A53T mutant human alpha-synuclein transgenic mice. *J Neuropathol Exp Neurol*. 2014;73:1144–1151.
33. Aureli F, D'Amato M, Raggi A, et al. Quantitative characterization of silica nanoparticles by asymmetric flow field flow fractionation coupled with online multiangle light scaterring and ICP-MS/MS detection. *J Anal At Spectrom*. 2015;30:1266–1273.
34. Aureli F, D'Amato M, Raggi A, et al. (eds). *90-day oral toxicity study on SAS in rats: use of state-of-the art approaches for characterization of nanomaterial dispersion and tissue deposition.* Paper presented at: Second National Conference "Nanotechnologies and Nanomaterials in the Food Sector and Their Safety Assessment." April 29, 2016; Istituto Superiore di Sanità, Rome, Italy.
35. Alvarez YD, Fauerbach JA, Pellegrotti JV, et al. Influence of gold nanoparticles on the kinetics of alpha-synuclein aggregation. *Nano Lett*. 2013;13:6156–6163.
36. Naudet N, Antier E, Gaillard D, et al. Oral exposure to paraquat triggers earlier expression of phosphorylated alpha-synuclein in the enteric nervous system of A53T mutant human alpha-synuclein transgenic mice. *J Neuropathol Exp Neurol*. 2017;76:1046–1057.
37. Cuchard P, Cuchard R, Rotman S, et al. Renal amyloidosis. *Rev Med Suisse*. 2012;8:446–451.
38. Satoskar AA, Burdge K, Cowden DJ, et al. Typing of amyloidosis in renal biopsies: diagnostic pitfalls. *Arch Pathol Lab Med*. 2007;131:917–922.
39. Picken MM, Herrera GA. The burden of "sticky" amyloid: typing challenges. *Arch Pathol Lab Med*. 2007;131:850–851.
40. Real de Asua D, Costa R, Galvan JM, et al. Systemic AA amyloidosis: epidemiology, diagnosis, and management. *Clin Epidemiol*. 2014;6:369–377.
41. Nienhuis HL, Bijzet J, Hazenberg BP. The prevalence and management of systemic amyloidosis in western countries. *Kidney Dis (Basel)*. 2016;2:10–19.
42. Sipe JD, Benson MD, Buxbaum JN, et al. Amyloid fibril proteins and amyloidosis: chemical identification and clinical classification International Society of Amyloidosis. 2016 Nomenclature Guidelines. *Amyloid*. 2016;23:209–213.
43. Subramanian S, Javaid MM. Kidney disease of unknown cause in agricultural laborers (KDUCAL) is a better term to describe regional and endemic kidney diseases such as uddanam nephropathy. *Am J Kidney Dis*. 2017;69:552.
44. Weaver VM, Fadrowski JJ, Jaar BG. Global dimensions of chronic kidney disease of unknown etiology (CKDu): a modern era environmental and/or occupational nephropathy? *BMC Nephrol*. 2015;16:145.
45. Gadde P, Sanikommu S, Manumanthu R, et al. Uddanam nephropathy in India:a challenge for epidemiologists. *Bull World Health Organ*. 2017;95:848–849.